Quarkonia suppression in PbPb collisions at sqrt[s_{NN}]=2.76 TeV

Vineet Kumar, Prashant Shukla, and Ramona Vogt

Quarkonia suppression in Pb+Pb collisions at $\sqrt{s_{NN}} = 2.76$ TeV

Vineet Kumar,[1,2] Prashant Shukla,[1,2,*] and Ramona Vogt[3,4]

[1]*Nuclear Physics Division, Bhabha Atomic Research Center, Mumbai, India*

[2]*Homi Bhabha National Institute, Anushakti Nagar, Mumbai, India*

[3]*Nuclear and Chemical Sciences Division,*

Lawrence Livermore National Laboratory, Livermore, CA 94551, USA

[4]*Physics Department, University of California, Davis, CA 95616, USA*

Abstract

We estimate the modification of quarkonia yields due to different processes in the medium produced in Pb+Pb collisions at LHC energy. The quarkonia and heavy flavour cross sections calculated up to next-to-leading order (NLO) are used in the study. Shadowing corrections are obtained with the NLO EPS09 parametrization. A kinetic model is employed which incorporates quarkonia suppression inside a QGP, suppression due to hadronic comovers, and regeneration from charm pairs. The quarkonia dissociation cross section due to gluon collisions has been considered and the regeneration rate has been obtained using the principle of detailed balance. The modification in quarkonia yields due to collisions with hadronic comovers has been estimated assuming that the comovers are pions. The manifestations of these effects on the nuclear modification factors for both J/ψ and Υ in different kinematic regions has been demonstrated for Pb+Pb collisions at $\sqrt{s_{NN}}$ = 2.76 TeV in comparison with the measurements. Both the suppression and regeneration due to a deconfined medium strongly affect the low and intermediate p_T range. The large observed suppression of J/ψ at $p_T > 10$ GeV/c exceeds the estimates of suppression by gluon dissociation.

* pshukla@barc.gov.in

I. INTRODUCTION

Heavy-ion collisions at relativistic energies are performed to create and characterize quark gluon plasma (QGP), a phase of strongly-interacting matter at high energy density where quarks and gluons are no longer bound within hadrons. The quarkonia states (J/ψ and Υ) have been some of the most popular tools since their suppression was proposed as a signal of QGP formation [1]. The understanding of these probes has evolved substantially via measurements through three generations of experiments: the SPS (at CERN), RHIC (at BNL) and the LHC (at CERN) and by a great deal of theoretical activity. (For recent reviews see Refs. [2–4].) Quarkonia are produced early in the heavy-ion collisions and, if they evolve through the deconfined medium, their yields should be suppressed in comparison with those in pp collisions. The first such measurement was the 'anomalous' J/ψ suppression discovered at the SPS which was considered to be a hint of QGP formation. The RHIC measurements showed almost the same suppression at a much higher energy contrary to expectation [4, 5]. Such an observation was consistent with the scenario that, at higher collision energies, the expected greater suppression is compensated by J/ψ regeneration through recombination of two independently-produced charm quarks [6]. Since the LHC first performed Pb+Pb collisions at $\sqrt{s_{NN}} = 2.76$ TeV, a wealth of quarkonia results have become available [7, 8]. The CMS experiment carries out J/ψ measurements at high transverse momentum ($p_T > 6.5$ GeV/c). The nuclear modification factor R_{AA} of these high p_T prompt J/ψ decreases with increasing centrality [9, 10] showing moderate suppression even in the most peripheral collisions. Moreover R_{AA} is found to be nearly independent of p_T (above 6.5 GeV/c), showing that the J/ψ remains suppressed, even at very high p_T, up to ~ 16 GeV/c. By comparing with the STAR results [11] at RHIC it follows that the suppression of high p_T J/ψ has increased with collision energy. The ALICE J/ψ results [12] cover low p_T and have little or no centrality dependence. The ALICE J/ψ suppression decreases substantially with decreasing p_T. When compared with the PHENIX forward rapidity measurement at RHIC [5], it suggests that low p_T J/ψ's are less suppressed at the LHC. These observations suggest J/ψ regeneration at low p_T by recombination of independently-produced charm pairs. At LHC energies, the Υ states are produced with good statistics. The CMS measurements [13, 14] reveal that the higher Υ states are more suppressed relative to the ground state, a phenomenon known as sequential suppression. The ALICE measurements [15] at forward

rapidity, $(2.5 \leq y^{\Upsilon} \leq 4.0)$ are consistent with CMS measurements at midrapidity, $|y^{\Upsilon}| \leq 2.4$.

Many models were developed for the modification of quarkonia due to different processes before the LHC startup. The suppression of quarkonia in a QGP is understood in terms of color screening models e.g. Ref. [1, 16] and, alternatively, in terms of quarkonium dissociation by collisions with gluons [17, 18]. Statistical models [6, 19] can estimate of the regeneration of quarkonia by charm quark pairs. The inverse of the gluon dissociation process can also be used to estimate regeneration [20]. The quarkonia yields in heavy-ion collisions are modified by non-QGP effects such as shadowing, due to the modification of the parton distribution functions inside the nucleus, and dissociation due to hadronic or comover interaction [21]. There have been many recent calculations to explain the LHC quarkonia results using a combination of the above frameworks [22, 23] as well as viscous hydrodynamics [24].

In this paper, we calculate J/ψ and Υ production and suppression in a kinetic model which includes dissociation due to thermal gluons, modification of the yields due to shadowing and due to collisions with comovers. Regeneration by thermal heavy quark pairs is also taken into account. Our goal is to obtain the nuclear modification factor of quarkonia as a function of transverse momentum and collision centrality and compare it to experimental data from CMS and ALICE.

II. THE PRODUCTION RATES AND COLD NUCLEAR MATTER EFFECTS

The heavy quark production cross section are calculated to NLO in pQCD using the CT10 parton densities [25]. The mass and scale parameters used for open and hidden heavy flavor production are obtained by fitting the energy dependence of open heavy flavor production to the measured total cross sections [26, 27]. Those obtained for open charm are $m_c = 1.27 \pm 0.09$ GeV, $\mu_F/m_{Tc} = 2.10^{+2.55}_{-0.85}$, and $\mu_R/m_{Tc} = 1.60^{+0.11}_{-0.12}$ [26]. The botttom quark mass and scale parameters are $m_b = 4.65 \pm 0.09$ GeV, $\mu_F/m_{Tb} = 1.40^{+0.75}_{-0.47}$, and $\mu_R/m_{Tb} = 1.10^{+0.26}_{-0.19}$ [27]. The quarkonium production cross sections are calculated in the color evaporation model with normalizations determined from fitting the scale parameter to the shape of the energy-dependent cross sections [26, 27]. The resulting uncertainty bands are smaller than those obtained with the fiducial parameters used in Ref. [28]. We note that the new results are within the uncertainties of those Ref. [28]. Indeed, the charm cross

TABLE I. Heavy quark and quarkonia production cross sections at $\sqrt{s_{NN}} = 2.76$ TeV. The cross sections are given per nucleon pair while N^{PbPb} gives the initial number of heavy quark pair/quarkonia per Pb+Pb event.

	$c\bar{c}$	J/ψ	$b\bar{b}$	Υ
σ_{pp}	$4.11^{+2.69}_{-2.50}$ mb	$21.6^{+10.6}_{-10.4}$ μb	$110.5^{+15.1}_{-14.2}$ μb	$0.22^{+0.07}_{-0.06}$ μb
σ_{PbPb}	$3.21^{+2.1}_{-1.95}$ mb	$16.83^{+8.26}_{-8.10}$ μb	$100.5^{+13.7}_{-12.9}$ μb	$0.199^{+0.063}_{-0.054}$ μb
N^{PbPb}	18.12^{+12}_{-11}	$0.0952^{+0.047}_{-0.046}$	$0.57^{+0.08}_{-0.07}$	$0.001123^{+0.0004}_{-0.0003}$

sections reported at the LHC agree better with the new values of the mass and scale than the central value of $m_c = 1.5$ GeV, $\mu_F/m_T = \mu_R/m_T = 1$. The central EPS09 NLO parameter set [29] is used to calculate the modifications of the parton distribution functions (nPDF) in Pb+Pb collisions, referred as cold nuclear matter (CNM) effects. The CNM uncertainty is calculated by adding the EPS09 NLO uncertainties in quadrature. The production cross sections for heavy flavor and quarkonia at $\sqrt{s_{NN}} = 2.76$ TeV [30] are given in Table I. The yields in a minimum bias Pb+Pb event is obtained from the per nucleon cross section, σ_{PbPb}, in Table I, as

$$N = \frac{A^2 \sigma_{\mathrm{PbPb}}}{\sigma_{\mathrm{PbPb}}^{\mathrm{tot}}} \ . \tag{1}$$

At 2.76 TeV, the total Pb+Pb cross section, $\sigma_{\mathrm{PbPb}}^{\mathrm{tot}}$, is 7.65 b [31].

III. MODIFICATION OF QUARKONIA IN THE PRESENCE OF QGP

In the kinetic approach [20], the proper time τ evolution of the quarkonia population N_Q is given by the rate equation

$$\frac{dN_Q}{d\tau} = -\lambda_D \rho_g N_Q + \lambda_F \frac{N_{q\bar{q}}^2}{V(\tau)}, \tag{2}$$

where $V(\tau)$ is the volume of the deconfined spatial region and $N_{q\bar{q}}$ is the number of initial heavy quark pairs produced per event depending on the centrality defined by the number of participants N_{part}. The λ_D is the dissociation rate obtained by the dissociation cross section averaged over the momentum distribution of gluons and λ_F is the formation rate obtained by the formation cross section averaged over the momentum distribution of heavy quark

pair q and $\bar{q}$. ρ_g is the density of thermal gluons. The number of quarkonia at freeze-out time τ_f is given by the solution of Eq. (2),

$$N_Q(p_T) = S(p_T)\,N_Q^{\text{PbPb}}(p_T) + N_Q^F(p_T). \tag{3}$$

Here $N_Q^{\text{PbPb}}(p_T)$ is the number of initially-produced quarkonia (including shadowing) as a function of p_T and $S(p_T)$ is their survival probability from gluon collisions at freeze-out,

$$S(p_T) = \exp\left(-\int_{\tau_0}^{\tau_f} f(\tau)\lambda_D(T,p_T)\,\rho_g(T)\,d\tau\right). \tag{4}$$

The temperature $T(\tau)$ and the QGP fraction $f(\tau)$ evolve from initial time τ_0 to freeze-out time τ_f due to expansion of the QGP. The initial temperature and the evolution is dependent on collision centrality N_{part}. $N_Q^F(p_T)$ is the number of regenerated quarkonia per event,

$$N_Q^F(p_T) = S(p_T)N_{q\bar{q}}^2 \int_{\tau_0}^{\tau_f} \frac{\lambda_F(T,p_T)}{V(\tau)\,S(\tau,p_T)}d\tau. \tag{5}$$

The nuclear modification factor (R_{AA}) can be written as

$$R_{AA}(p_T) = S(p_T)\,R(p_T) + \frac{N_Q^F(p_T)}{N_Q^{pp}(p_T)}. \tag{6}$$

Here $R(p_T)$ is the shadowing factor. R_{AA} as a function of collision centrality, including regeneration, is

$$R_{AA}(N_{\text{part}}) = \frac{\int_{p_T\,\text{cut}} N_Q^{pp}(p_T)S(p_T)\,R(p_T)dp_T}{\int_{p_T\,\text{cut}} N_Q^{pp}(p_T)dp_T} + \frac{\int_{p_T\,\text{cut}} N_Q^F(p_T)dp_T}{\int_{p_T\,\text{cut}} N_Q^{pp}(p_T)dp_T} \tag{7}$$

Here $p_{T\text{ cut}}$ defines the p_T range for a given experimental acceptance. $N_Q^{pp}(p_T)$ is the unmodified p_T distribution of quarkonia obtained by NLO calculations and scaled to a particular centrality of the Pb+Pb collisions.

The evolution of the system for each centrality bin is governed by an isentropic cylindrical expansion with volume element

$$V(\tau) = \tau\,\pi\,(R + \frac{1}{2}a_T\,\tau^2)^2, \tag{8}$$

where $a_T = 0.1\,c^2$ fm^{-1} is the transverse acceleration [22]. The initial transverse size, R, as a function of centrality is

$$R(N_{\text{part}}) = R_{0-5\%}\sqrt{\frac{N_{\text{part}}}{(N_{\text{part}})_{0-5\%}}}, \tag{9}$$

5

where $R_{0-5\%} = 0.96\,R_{\mathrm{Pb}}$ and R_{Pb} is the radius of the lead nucleus. The evolution of entropy density for each centrality is obtained by entropy conservation, $s(T)\,V(\tau) = s(T_0)\,V(\tau_0)$. The equation of state (EOS) obtained from Lattice QCD, along with a hadronic resonance gas, [32] is used to obtain the temperature as a function of proper time τ. The initial entropy density for each centrality is calculated using

$$s(\tau_0) = s(\tau_0)|_{0-5\%} \left(\frac{dN/d\eta}{N_{\mathrm{part}}/2} \right) \left(\frac{dN/d\eta}{N_{\mathrm{part}}/2} \right)_{0-5\%}^{-1}. \tag{10}$$

Measured values of $(dN/d\eta)/(N_{\mathrm{part}}/2)$ as a function of N_{part} [33, 34] are used in the calculations. The initial entropy density, $s(\tau_0)|_{0-5\%}$, for 0-5% centrality is

$$s(\tau_0)|_{0-5\%} = \frac{a_m}{V(\tau_0)|_{0-5\%}} \left(\frac{dN}{d\eta} \right)_{0-5\%}. \tag{11}$$

Here $a_m\ (=5)$ is a constant which relates the total entropy to the total multiplicity $dN/d\eta$. It is obtained from hydrodynamic calculations [35]. We estimate the initial temperature, T_0, in the 0-5% most central collisions from the total multiplictity in the rapidity region of interest, assuming that the initial time is $\tau_0 = 0.3$ fm/c over all rapidity. The total multiplicity in a given rapidity region is 3/2 times the charged particle multiplicity in Pb+Pb collisions at 2.76 TeV. With the lattice EOS, at midrapidity, with $(dN_{\mathrm{ch}}/d\eta)_{0-5\%} = 1600$ [33, 34], we find $T_0 = 0.484$ GeV. Likewise, at forward rapiidity, $2.5 \leq y \leq 4$ [36], $T_0 = 0.427$ GeV. The (proper) time evolution of temperature is shown in Fig. 1(a) and that of QGP fraction in Fig. 1(b), in the case of the most central (0-5%) collisions. Here we compare the evolution obtained with longitudinal and cylindrical expansions using both a first order and the lattice EOS. For the first order EOS, $T_c = 0.170$ GeV. The QGP fraction goes from 1 to 0 at T_c assuming a mixed phase of QGP and hadrons. The QGP fraction in case of lattice EOS governs the number of degrees of freedom, decided by the entropy density. It is fixed to unity above an entropy density corresponding to a 2-flavour QGP and fixed to zero below entropy density for a hot resonance gas. The freeze out temperature in all cases is $T_f = 0.140$ GeV.

A. Dissociation Rate

In the color dipole approximation, the gluon dissociation cross section as function of gluon energy, q^0, in the quarkonium rest frame is [17]

$$\sigma_D(q^0) = \frac{8\pi}{3} \frac{16^2}{3^2} \frac{a_0}{m_q} \frac{(q^0/\epsilon_0 - 1)^{3/2}}{(q^0/\epsilon_0)^5}, \tag{12}$$
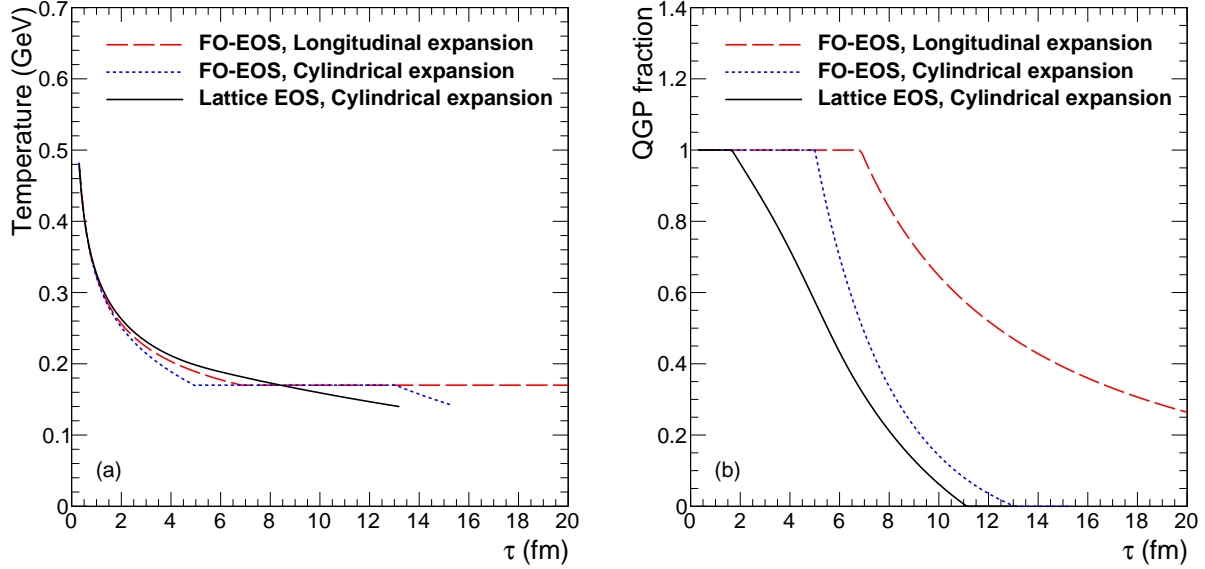
6

FIG. 1. (Color online) (a) Temperature and (b) QGP fraction in the system as a function of proper time τ in case of the most central (0-5%) collisions for longitudinal and cylindrical expansions using first order and lattice equation of state .

where ϵ_0 is the quarkonia binding energy and m_q is the charm/bottom quark mass and $a_0 = 1/\sqrt{m_q \epsilon_0}$. The values of ϵ_0 are taken as 0.64 and 1.10 GeV for the ground states, J/ψ and $\Upsilon(1S)$, respectively [37]. For the first excited state of bottomonia, $\Upsilon(2S)$, we use dissociation cross section from Ref. [38].

Figure 2 shows the gluon dissociation cross sections of J/ψ and $\Upsilon(1S)$ as a function of gluon energy. The dissociation cross section is zero when the gluon energy is less than the binding energy of the quarkonia. It increases with gluon energy and reaches a maximum at 1.2 (1.5) GeV for J/ψ ($\Upsilon(1S)$). At higher gluon energies, the interaction probability decreases. The gluon energy q^0 is related to the square of the center of mass energy s, of the quarkonium-gluon system by

$$q^0 = \frac{s - M_Q^2}{2\,M_Q} \tag{13}$$

where $s = M_Q^2 + 2p_g\sqrt{M_Q^2 + p^2} - 2p_g\,p\cos\theta$, and M_Q and p are mass and momentum of quarkonium and θ is angle between the quarkonium and the gluon. We calculate the dissociation rate as a function of quarkonium momentum by integrating the dissociation cross
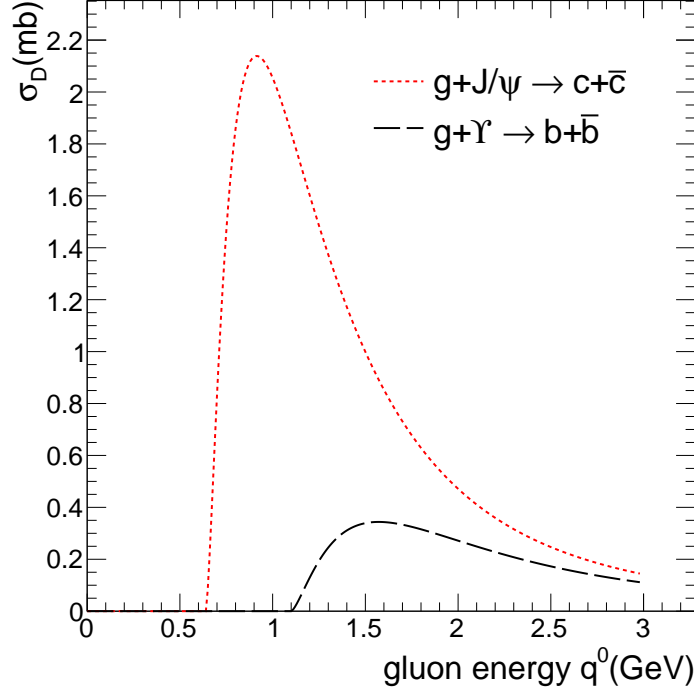
7

FIG. 2. (Color online) Gluon dissociation cross section of quarkonia as a function of gluon energy (q^0) in quarkonia rest frame.

section over thermal gluon momentum distribution $f_g(p_g)$,

$$\lambda_D \rho_g = \langle \sigma v_{\text{rel}} \rangle \, \rho_g = \frac{g_g}{(2\pi)^3} \int d^3 p_g \, f_g(p_g) \, \sigma_D(s) v_{\text{rel}}(s)$$
$$= \frac{g_g}{(2\pi)^3} \int dp_g 2\pi p_g^2 f_g(p_g) \int d\cos\theta \, \sigma_D(s) \, v_{\text{rel}}(s), \tag{14}$$

where $\sigma_D(s) = \sigma_D(q^0(s))$. The relative velocity, v_{rel}, between the quarkonium and the gluon is

$$v_{\text{rel}} = \frac{s - M_Q^2}{2p_g \sqrt{M_Q^2 + p^2}}. \tag{15}$$

The J/ψ gluon dissociation rates as a function of T are shown in Fig. 3(a) and as a function of p_T in Fig. 3(b). The dissociation rate increases with temperature due to the increase in gluon density. The dissociation rate is maximum when the quarkonium is at rest and decreases with p_T.
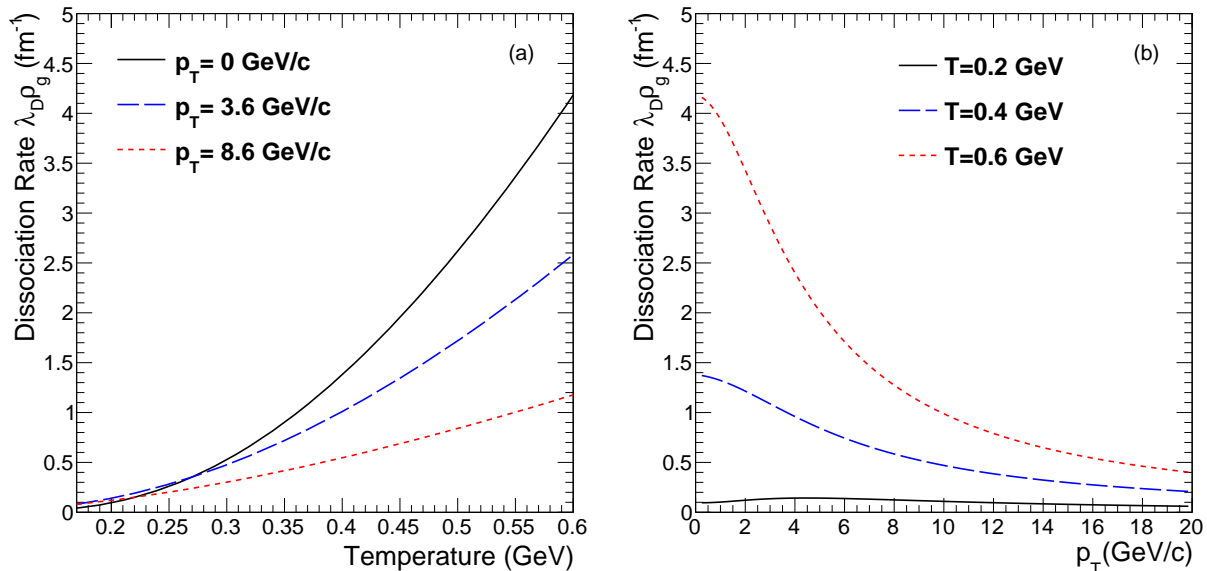
8

FIG. 3. (Color online) Gluon dissociation rate of J/ψ as a function of (a) temperature and (b) transverse momentum.

B. Formation Rate

We can calculate the formation cross section from the dissociation cross section using detailed balance [20, 39],

$$\sigma_F = \frac{48}{36}\,\sigma_D(q^0)\frac{(s-M_Q^2)^2}{s(s-4m_q^2)}. \tag{16}$$

The formation rate of quarkonium with momentum $\mathbf{p}$ can be written as

$$\frac{d\lambda_F}{d\mathbf{p}} = \int d^3p_1\, d^3p_2\, \sigma_F(s)\, v_{\rm rel}(s)\, f_q(p_1)\, f_{\bar{q}}(p_2)\, \delta(\mathbf{p}-(\mathbf{p_1}+\mathbf{p_2})). \tag{17}$$

Here $f_{q/\bar{q}}(p)$ are taken as thermal distribution function of $q/\bar{q}$ which are normalized to one, $\int f_q(p)d^3p = 1$ and $v_{\rm rel}$ is relative velocity of the $q\bar{q}$ quark pair,

$$v_{\rm rel} = \frac{\sqrt{(p_1.p_2)^2 - m_q^4}}{E_1\,E_2}. \tag{18}$$

Here $p_1 = (E_1, \mathbf{p_1})$ and $p_2 = (E_2, \mathbf{p_2})$ are the four momenta of the heavy quark and antiquark respectively. Figure 4 (a) shows the variation of the formation rate as a function of T and Fig. 4 (b) shows as a function of $J/\psi\ p_T$. The J/ψ generated from recombination of uncorrelated heavy quark pairs will have softer p_T distributions than those of J/ψ's coming from the initial hard scatterings. Thus the effect of recombination will be important only at low p_T.
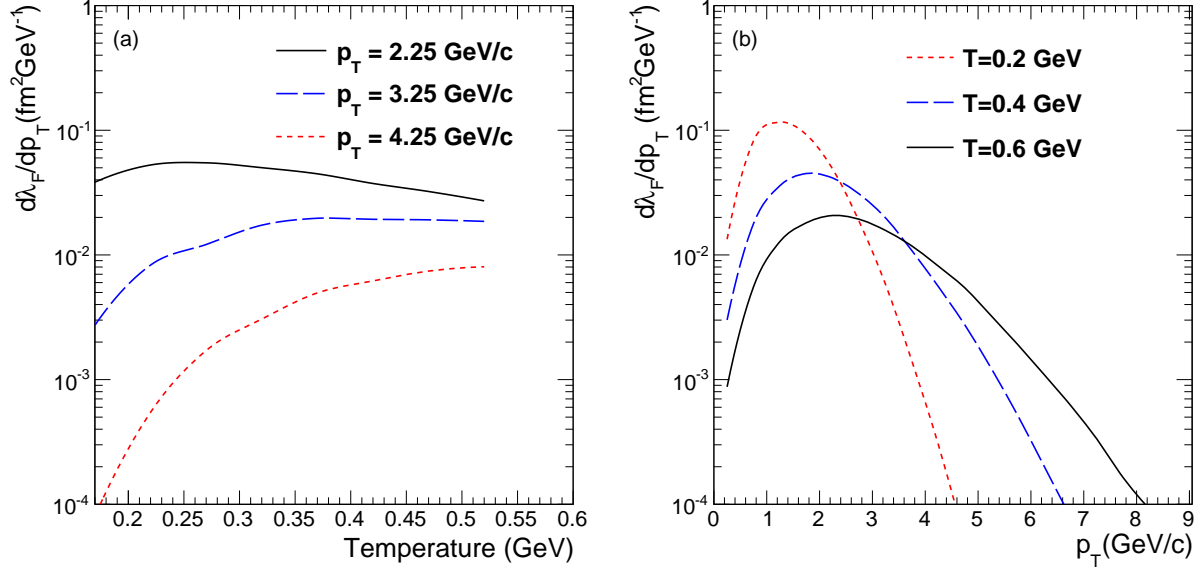
9

FIG. 4. (Color online) Formation rate of J/ψ as a function of (a) temperature and (b) transverse momentum.
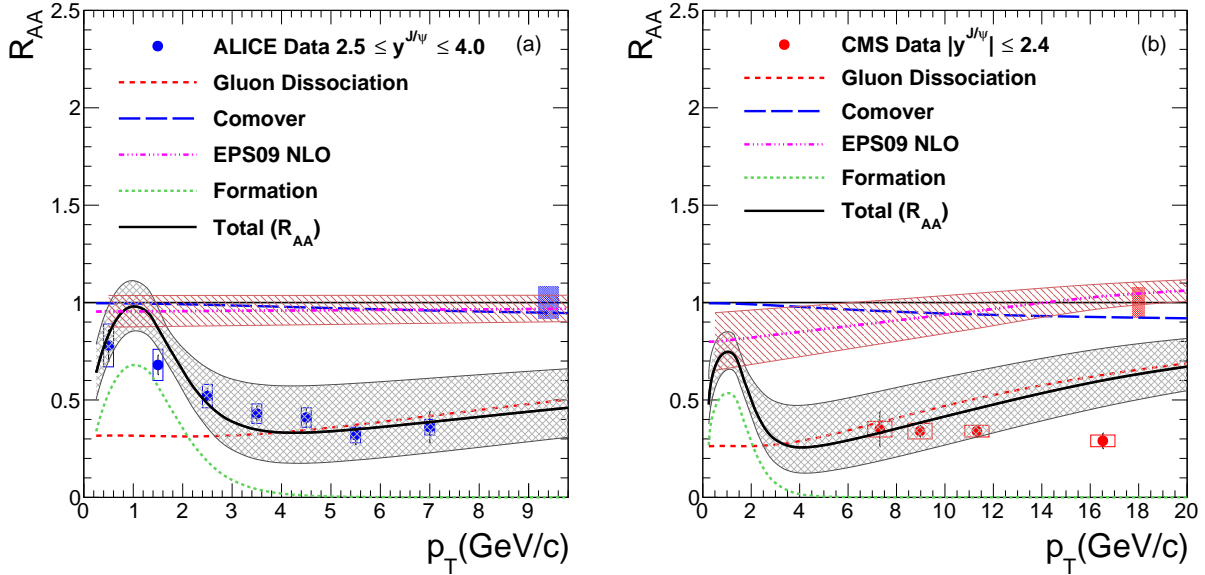

FIG. 5. (Color online) Calculated nuclear modification factor (R_{AA}) as a function of J/ψ transverse momentum compared with (a) ALICE and (b) CMS measurements.

IV. HADRONIC COMOVERS

The suppression of quarkonia by comoving pions can be calculated by folding the quarkonium-pion dissociation cross section $\sigma_{\pi Q}$ over thermal pion distributions [40]. It
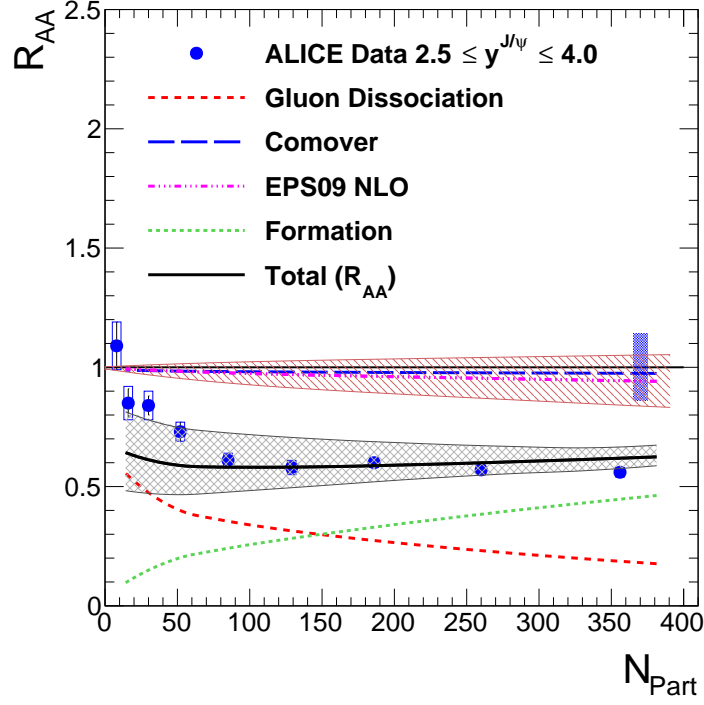
10

FIG. 6. (Color online) Calculated nuclear modification factor (R_{AA}) compared with ALICE measurements at LHC.
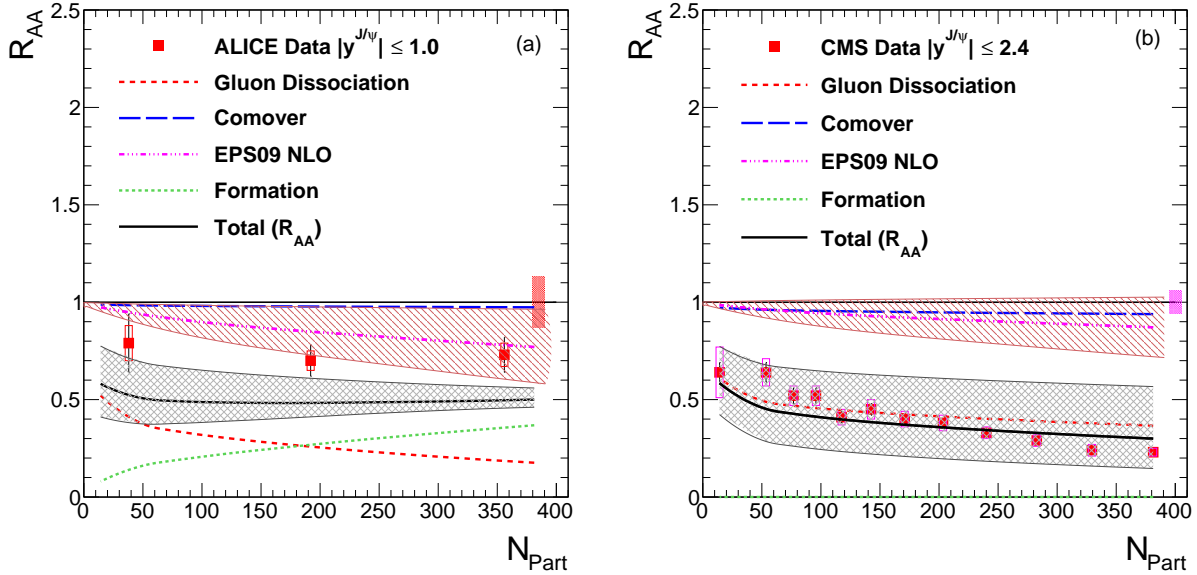

FIG. 7. (Color online) Calculated nuclear modification factor (R_{AA}) compared with (a) ALICE and (b) CMS measurements at midrapidity. The regeneration for the CMS high p_T measurement is negligible in comparison to the low p_T ALICE measurement.
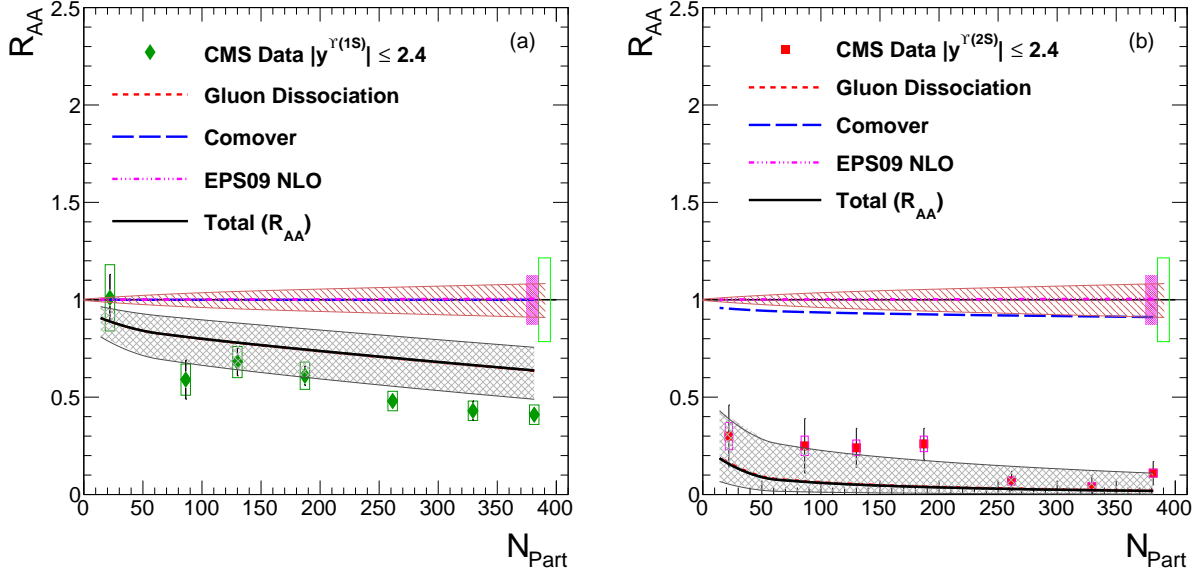
11

FIG. 8. (Color online) Calculated nuclear modification factor (R_{AA}) compared with CMS (a) $\Upsilon(1S)$ and (b) $\Upsilon(2S)$ measurements. Regeneration is assumed to be negligible.
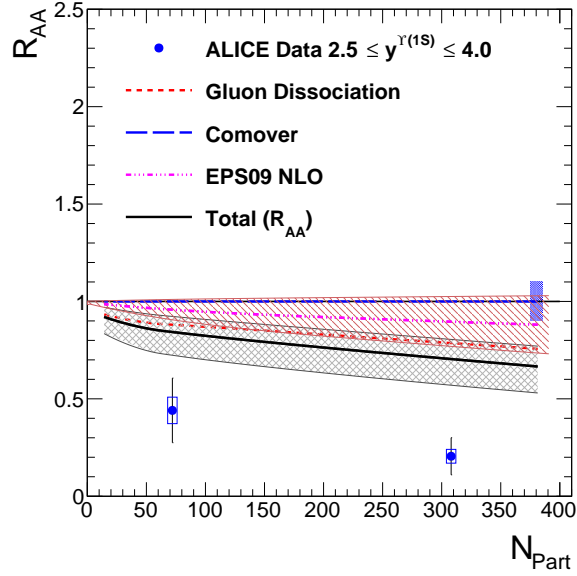

FIG. 9. (Color online) Calculated nuclear modification factor (R_{AA}) compared with ALICE $\Upsilon(1S)$ measurement in forward rapidity.

is expected that at LHC energies, the comover cross section will be small [41]. The pion-quarkonia cross section is calculated by convoluting the gluon-quarkonia cross section σ_D
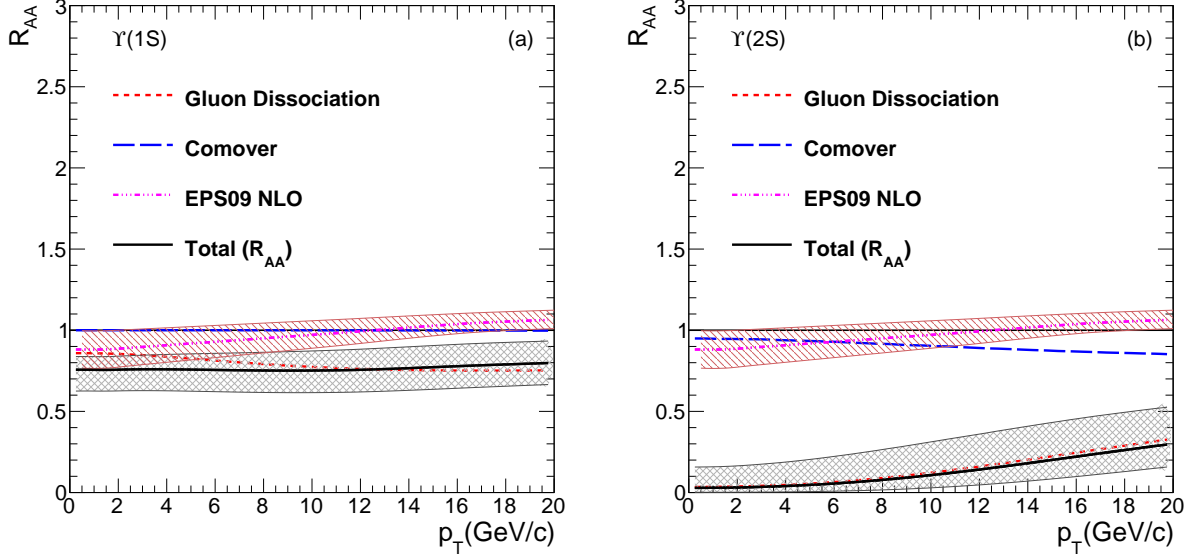
FIG. 10. (Color online) Calculated nuclear modification factor (R_{AA}) as a function of Υ transverse momentum.

over the gluon distribution inside the pion [38],

$$\sigma_{\pi Q}(p_\pi) = \frac{p_+^2}{2(p_\pi^2 - m_\pi^2)} \int_0^1 dx\, G(x)\, \sigma_D(xp_+/\sqrt{2}), \qquad (19)$$

where $p_+ = (p_\pi + \sqrt{p_\pi^2 - m_\pi^2})/\sqrt{2}$. The gluon distribution, $G(x)$, inside a pion is given by the GRV parameterization [42]. The pion momentum p_π is related to center of mass energy $\sqrt{s}$ of pion-J/ψ system by $p_\pi = (s - M_Q^2 - m_\pi^2)/(2M_Q)$. The dissociation rate λ_{D_π} can be written as

$$\lambda_{D_\pi}\, \rho_\pi = \frac{g_\pi}{(2\pi)^3} \int d^3p_\pi f_\pi(p)\sigma_{\pi Q}(s)v_{\rm rel}(s) \qquad (20)$$
$$= \frac{g_\pi}{(2\pi)^3} \int dp_\pi\, 2\pi p_\pi^2 f_\pi(p_\pi) \int d\cos\theta\, \sigma_{\pi Q}(s)\, v_{\rm rel}(s)\Theta(s - 4m_D^2),$$

where $f_\pi(p_\pi, T)$ is the thermal pion distribution. The pion density ρ_π is

$$\rho_\pi = \frac{g_\pi}{(2\pi)^3} \int d^3p_\pi\, f_\pi(p_\pi). \qquad (21)$$

The survival probability from pion collisions at freeze-out time τ_f is written as

$$S_\pi(p_T) = \exp\left(-\int_{\tau_0}^{\tau_f} d\tau\, (1 - f(\tau))\lambda_{D_\pi}(T, p_T)\, \rho_\pi(T)\right). \qquad (22)$$

The hadronic fraction $(1-f(\tau))$ is zero in QGP phase. The probability $S_\pi(p_T)$ multiplies $S(p_T)$ in Eq. (6).

13

V. RESULTS AND DISCUSSION

Figure 5(a) shows the contributions to the nuclear modification factor, R_{AA}, for the J/ψ as a function of p_T compared with ALICE measurements [12]. Figure 5(b) shows the same for the CMS high p_T measurements [10]. At low p_T, regeneration of J/ψ is the dominant process and this seems to be the reason for the enhancement of J/ψ in the ALICE low p_T data. The gluon suppression is also substantial at low p_T and reduces as we move to high p_T. Both of these processes (regeneration and dissociation) due to the presence of QGP are at play at low and intermediate p_T. The high p_T suppression ($p_T > 10$ GeV/c) of J/ψ measured by CMS is greater than that due to dissociation by gluons in the QGP. We note that at the highest p_T values from CMS, $p_T \gg M_Q$, and energy loss might play a similar role for the J/ψ at this p_T as it does for open charm. So the large suppression observed in the high p_T region may be due to energy loss inside the QGP. The dominant sources of the uncertainties come from the gluon-quarkonia cross section (σ_D) and initial temperature T_0. We vary the quarkonium-gluon cross section by $\pm 50\%$ around the calculated value to obtain the variation in the final R_{AA} calculations. The initial temperature is obtained using measured charged particle density and assuming τ_0 0.3 fm/c. We vary τ_0 in the range 0.1 $< \tau_0 < 0.6$ fm/c to quantify the uncertainty in R_{AA} corresponding to variation in the initial temperature from +45 % to - 20 %. Both of these uncertainties are added in quadrature to obtain the final uncertainty band around the central value. The variation of τ_0 and σ_D results in bands on the gluon dissociation and formation curves. At low p_T the uncertainty in the total R_{AA} is driven by the formation while at higher p_T, when gluon dissociation is dominant, the uncertainty reflects that component. The uncertainty in the CNM effect is not included in the R_{AA} uncertainty band since the CNM effects are not dominant.

We have also calculated R_{AA} as a function of collision centrality (system size). Figure 6 shows different contributions to the J/ψ nuclear modification factor as a function of system size, along with the ALICE forward rapidity measurements [12]. Figure 6 indicates that J/ψ's are increasingly suppressed by the QGP when the system size grows. Since the number of regenerated J/ψ's also grows, the nuclear modification factor remains flat for most of the centrality range. Figure 7 (a) shows the J/ψ nuclear modification factor along with the ALICE measurement at midrapidity [12]. Similar to forward rapidity, the nuclear modification factor is flat in the measured range of N_{part} due to the competitive effects of

14

gluon dissociation and regeneration. Our calculations reproduce the measured data within uncertainty. Figure 7 (b) shows the same for $p_T \geq 6.5$ GeV/c, measured by CMS experiment [10]. The CMS centrality dependence of the J/ψ R_{AA} is well described by the model. Most of the contribution to the CMS data comes from J/ψ's with $6.5 < p_T < 10$ GeV/c where the suppression is predominantly due to gluon dissociation.

Figure 8 (a) demonstrates the contributions from different processes to the centrality dependence of the Υ(1S) nuclear modification factor, along with the midrapidity data from CMS [14]. The calculations underestimate the suppression but reproduce the shape of centrality dependence. This may be due to the feed down effects from the excited states. Figure 8 (b) shows the same for the Υ(2S) nuclear modification factor along with the CMS measurements at midrapidity. The excited Υ(2S) states are highly suppressed. The effect of regeneration, not shown, is negligible for the Υ states. Figure 9 shows the forward rapidity ALICE measurement of the Υ(1S) nuclear modification factor [15] along with our calculations. The suppression due to thermal gluon dissociation is smaller than the measured suppression which may be due to the effect of feed down from the Υ(2S) and higher states. However the measurement is consistent with the suppression of Υ(2S) and Υ(3S) contribution, along with suppression of the Υ(1S) by gluon dissociation. Figure 10 (a) shows the contributions from different processes to the Υ(1S) nuclear modification factor as a function of transeverse momentum. The calculated R_{AA} shows weak dependence on p_T a trend similar to recently reported measurements of Υ(1S) suppression by CMS Collaboration [43]. Our calculations show less suppression than data which may be due to the effect of feeddowns from higher states. Figure 10 (b) shows the same for the Υ(2S) which shows almost the same suppression as seen in the data [43].

VI. SUMMARY

We have carried out detailed calculations of the J/ψ and Υ modifications in Pb+Pb collisions at LHC. The quarkonia and heavy flavour cross sections calculated up to NLO are used in the study. Shadowing corrections are obtained with the EPS09 NLO parametrization. A kinetic model is employed which incorporates quarkonia suppression inside QGP, suppression due to hadronic comovers and regeneration from charm pairs. The dissociation and formation rates have been studied as a function of medium temperature and transverse

momentum. The nuclear modification factors for J/ψ and Υ as a function of centrality and transverse momentum have been compared to the measurements in Pb+Pb collisions at $\sqrt{s_{NN}} = 2.76$ TeV. At low p_T, regeneration of J/ψ is the dominant process and this seems to be the process for the enhancement of J/ψ in the ALICE low p_T data. Gluon dissociation is also substantial at low p_T and becomes small as we move to high p_T. Both of these processes (regeneration and dissociation) due to the presence of QGP affec the yields of quarkonia at low and intermediate p_T. The high p_T suppression ($p_T > 10$ GeV/c) of J/ψ measured by CMS is far more than expected due to the dissociation by gluons in QGP. The centrality dependence of nuclear modification indicates that J/ψ's are increasingly suppressed when system size grows. Since the number of regenerated J/ψ's also grows, the nuclear modification factor of low p_T measurements (ALICE case) remains flat for most of the centrality region. The centrality dependence of R_{AA} for high p_T J/ψ's is also well described by the model. The centrality dependence of suppression of Υ states are reproduced by model calculations. Feed down corrections seems to be important for $\Upsilon(1S)$.

VII. ACKNOWLEDGEMENT

---

[1] T. Matsui and H. Satz, "J/ψ Suppression by Quark-Gluon Plasma Formation", Phys. Lett. B **178**, 416 (1986).

[2] J. Schukraft, "Heavy Ion Physics at the LHC: What's new ? What's next ?", arXiv:1311.1429 [hep-ex].

[3] L. Kluberg and H. Satz, "Color Deconfinement and Charmonium Production in Nuclear Collisions," arXiv:0901.3831 [hep-ph].

[4] N. Brambilla, S. Eidelman, B. K. Heltsley, R. Vogt, G. T. Bodwin, E. Eichten, A. D. Frawley

and A. B. Meyer *et al.*, "Heavy quarkonium: progress, puzzles, and opportunities," Eur. Phys. J. C **71**, 1534 (2011).

[5] A. Adare *et al.* [PHENIX Collaboration], "J/ψ suppression at forward rapidity in Au+Au collisions at $\sqrt{s_{NN}} = 200$ GeV," Phys. Rev. C **84**, 054912 (2011).

[6] A. Andronic, P. Braun-Munzinger, K. Redlich and J. Stachel, "Statistical hadronization of charm in heavy ion collisions at SPS, RHIC and LHC," Phys. Lett. B **571**, 36 (2003).

[7] B. Muller, J. Schukraft and B. Wyslouch, "First Results from Pb+Pb collisions at the LHC," Ann. Rev. Nucl. Part. Sci. **62**, 361 (2012).

[8] P. Shukla [CMS Collaboration], "Overview of quarkonia and heavy flavour measurements by CMS," arXiv:1405.3810 [nucl-ex].

[9] S. Chatrchyan *et al.* [CMS Collaboration], "Suppression of non-prompt J/ψ, prompt J/ψ, and Y(1S) in Pb+Pb collisions at $\sqrt{s_{NN}} = 2.76$ TeV," JHEP **1205**, 063 (2012).

[10] C. Mironov [CMS Collaboration], "Overview of results on heavy flavour and quarkonia from the CMS Collaboration," Nucl. Phys. A **904-905**, 194c (2013).

[11] Z. Tang [STAR Collaboration], "J/ψ production and correlation in p+p and Au+Au collisions at STAR," J. Phys. G **38**, 124107 (2011).

[12] B. B. Abelev *et al.* [ALICE Collaboration], "Centrality, rapidity and transverse momentum dependence of J/ψ suppression in Pb-Pb collisions at $\sqrt{s_{NN}}$=2.76 TeV," Phys. Lett. **743**, 314 (2014).

[13] S. Chatrchyan *et al.* [CMS Collaboration], "Indications of suppression of excited Υ states in PbPb collisions at $\sqrt{S_{NN}} = 2.76$ TeV," Phys. Rev. Lett. **107**, 052302 (2011).

[14] S. Chatrchyan *et al.* [CMS Collaboration], "Observation of sequential Upsilon suppression in PbPb collisions," Phys. Rev. Lett. **109**, 222301 (2012).

[15] B. B. Abelev *et al.* [ALICE Collaboration], "Suppression of Υ(1S) at forward rapidity in Pb-Pb collisions at $\sqrt{s_{NN}} = 2.76$ TeV," arXiv:1405.4493 [nucl-ex].

[16] A. Abdulsalam and P. Shukla, "Suppression of bottomonia states in finite size quark gluon plasma in PbPb collisions at Large Hadron Collider," Int. J. Mod. Phys. A **28**, 1350105 (2013).

[17] G. Bhanot and M. E. Peskin, "Short Distance Analysis for Heavy Quark Systems. 2. Applications," Nucl. Phys. B **156**, 391 (1979).

[18] X. -M. Xu, D. Kharzeev, H. Satz and X. -N. Wang, "J/ψ suppression in an equilibrating parton plasma," Phys. Rev. C **53**, 3051 (1996).

[19] A. Andronic, P. Braun-Munzinger, K. Redlich and J. Stachel, "The statistical model in Pb-Pb collisions at the LHC," Nucl. Phys. A **904-905**, 535c (2013).

[20] R. L. Thews, M. Schroedter and J. Rafelski, "Enhanced J/ψ production in deconfined quark matter," Phys. Rev. C **63**, 054905 (2001).

[21] R. Vogt, "Cold Nuclear Matter Effects on J/ψ and Υ Production at the LHC," Phys. Rev. C **81**, 044903 (2010).

[22] X. Zhao and R. Rapp, "Medium Modifications and Production of Charmonia at LHC," Nucl. Phys. A **859**, 114 (2011).

[23] A. Emerick, X. Zhao and R. Rapp, "Bottomonia in the Quark-Gluon Plasma and their Production at RHIC and LHC," Eur. Phys. J. A **48**, 72 (2012).

[24] M. Strickland, "Thermal Υ(1S) and χ_{b1} suppression in $\sqrt{s_{NN}} = 2.76$ TeV Pb-Pb collisions at the LHC," Phys. Rev. Lett. **107**, 132301 (2011).

[25] H. L. Lai, M. Guzzi, J. Huston, Z. Li, P. M. Nadolsky, J. Pumplin and C.-P. Yuan, "New parton distributions for collider physics," Phys. Rev. D **82**, 074024 (2010).

[26] R. E. Nelson, R. Vogt and A. D. Frawley, 'Narrowing the uncertainty on the total charm cross section and its effect on the J/ψ cross section," Phys. Rev. C **87**, no. 1, 014908 (2013).

[27] R. Nelson, R. Vogt and A. D. Frawley, in preparation.

[28] M. Cacciari, P. Nason and R. Vogt, "QCD predictions for charm and bottom production at RHIC," Phys. Rev. Lett. **95**, 122001 (2005).

[29] K. J. Eskola, H. Paukkunen and C. A. Salgado, "EPS09: A New Generation of NLO and LO Nuclear Parton Distribution Functions," JHEP **0904**, 065 (2009).

[30] V. Kumar, P. Shukla and R. Vogt, "Components of the dilepton continuum in Pb+Pb collisions at $\sqrt{s_{NN}} = 2.76$ TeV," Phys. Rev. C **86**, 054907 (2012).

[31] S. Chatrchyan *et al.* [CMS Collaboration], "Observation and studies of jet quenching in PbPb collisions at nucleon-nucleon center-of-mass energy = 2.76 TeV," Phys. Rev. C **84**, 024906 (2011).

[32] P. Huovinen and P. Petreczky, "QCD Equation of State and Hadron Resonance Gas," Nucl. Phys. A **837**, 26 (2010).

[33] K. Aamodt *et al.* [ALICE Collaboration], "Centrality dependence of the charged-particle multiplicity density at mid-rapidity in Pb-Pb collisions at $\sqrt{s_{NN}} = 2.76$ TeV," Phys. Rev. Lett. **106**, 032301 (2011).

[34] S. Chatrchyan *et al.* [CMS Collaboration], "Dependence on pseudorapidity and centrality of charged hadron production in PbPb collisions at a nucleon-nucleon centre-of-mass energy of 2.76 TeV," JHEP **1108**, 141 (2011).

[35] E. V. Shuryak, "Two stage equilibration in high-energy heavy ion collisions," Phys. Rev. Lett. **68**, 3270 (1992).

[36] E. Abbas *et al.* [ALICE Collaboration], "Centrality dependence of the pseudorapidity density distribution for charged particles in Pb-Pb collisions at $\sqrt{s_{\mathrm{NN}}} = 2.76$ TeV," Phys. Lett. B **726**, 610 (2013).

[37] F. Karsch, M. T. Mehr and H. Satz, "Color Screening and Deconfinement for Bound States of Heavy Quarks," Z. Phys. C **37**, 617 (1988).

[38] F. Arleo, P. B. Gossiaux, T. Gousset and J. Aichelin, "Heavy quarkonium hadron cross section in QCD at leading twist," Phys. Rev. D **65**, 014005 (2002).

[39] R. L. Thews and M. L. Mangano, "Momentum spectra of charmonium produced in a quark-gluon plasma," Phys. Rev. C **73**, 014904 (2006).

[40] R. Vogt, M. Prakash, P. Koch and T. H. Hansson, "J/ψ Interactions With Hot Hadronic Matter," Phys. Lett. B **207**, 263 (1988).

[41] C. Lourenco, R. Vogt and H. K. Woehri, "Energy dependence of J/ψ absorption in proton-nucleus collisions," JHEP **0902**, 014 (2009).

[42] M. Glueck, E. Reya and A. Vogt, "Pionic parton distributions," Z. Phys. C **53**, 651 (1992).

[43] CMS Collaboration, CMS-PAS-HIN-15001 "https:// twiki.cern.ch/twiki/ bin/view/ CMSPublic/ PhysicsResultsHIN15001".